Plasmonic coupling effect in Ag nanocap-nanohole pairs for surface-enhanced Raman scattering

Xiaolei Wen[1], Zheng Xi[1], Xiaojin Jiao[2], Wenhai Yu[1], Guosheng Xue[3] , Douguo Zhang[1],Yonghua Lu[1], Pei Wang[1] ,Steve Blair[2] and Hai Ming[1]

1 Department of Optics and Optical Engineering, Anhui Key Laboratory of Optoelectronic Science and Technology, University of Science and Technology of China, Hefei, Anhui, P. R. China, 230026

2 Department of Electrical and Computer Engineering, University of Utah, Salt Lake City, UT 84112, USA

3 Department of Optics and Optical Engineering, Bio-laser Laboratory, University of Science and Technology of China, Hefei, Anhui, P. R. China, 230026

E-mail: wangpei@ustc.edu.cn

Abstract

A plasmonic coupling structure composed of Ag nanocap-nanohole pairs was fabricated through a novel and facile method. Both surface-enhanced Raman scattering (SERS) measurements and numerical simulations show that the cap-hole system produces much larger electric field enhancement and SERS signal than the isolated structures, which is due to the plasmonic coupling effect between the gap of the cap and the hole. Additionally, the plasmonic enhancement is sensitive to the gap size, which can be controlled by the Ag layer thickness during the evaporation process. A maximum enhancement factor of 1.1×10^8 can be obtained with optimized gap size.

Introduction

Surface-enhanced Raman scattering (SERS) is an effective analytical chemical sensing technique which continues to attract a great deal of research attention [1 2 3]. It is now well-known that the main contribution to SERS is the electromagnetic (EM) mechanism which relies on the generation of surface plasmons (SPs) in metallic nanostructures [4 5 6 7]. SPs can enhance the local EM fields on the metal surface and concentrate them into subwavelength volumes, resulting in dramatically enhanced Raman signals from adsorbates lying within these volumes. Moreover, several recent studies have shown that a nanoscale dielectric gap (typically 5-20nm) between adjacent metal structures can induce plasmonic coupling effects, which harness EM energy much more efficiently than the isolated structures [8 9 10 11]. The use of nanoscale plasmonic coupling gaps therefore provides a promising approach to realize highly efficient SERS platforms. However, the lack of convenient, reproducible and high-throughput fabrication methods for such SERS substrates has limited their widespread adoption.

In this paper we present a low-cost one-step method to fabricate a plasmonic coupling structure composed of Ag nanocap-nanohole pairs. We demonstrate that this structure can be employed as an efficient SERS substrate, providing an enhancement factor as high as 1.1×10^8. The plasmonic coupling effect of this structure is also investigated by experimental and numerical methods and is shown to be very sensitive

to the gap size, which can be precisely controlled.

In our experiments, we used a near-infrared (NIR) laser (785nm) as the excitation source for SERS measurement. NIR excitation is advantageous in single molecule detection and biomolecule application [12 13], as it can strongly decrease the background (fluorescence and Raman signal of the surrounding medium), penetrate deeper in biological tissues and lead to smaller photothermal damage to biomolecules because of its low photon energy. Additionally, NIR excitation is nonresonant for most molecules (including rhodamine 6G (R6G) used in our experiments), so it allows for the use of high excitation intensities without photo bleaching and ensures that the SERS signals are generated mostly from the electromagnetic (EM) mechanism.

Experimental details

The Ag nanocap-nanohole pairs were fabricated according to the procedure shown in Figure 1(a). First, commercially available 200 nm diameter polystyrene (PS) nanospheres were randomly dispersed on clean glass substrates, followed by baking at 85 ℃ for 30 min. Then an Ag layer was thermal evaporated at normal incidence onto the substrates. The top of each PS nanosphere was covered with Ag as well as the surface of the glass substrate around it, resulting in an Ag nanocap on each PS nanosphere with a Ag nanohole underneath it [14 15]. Scanning electron microscopy (SEM) images of such Ag nanocap-nanohole pairs are shown in Figure 1(c). A zoomed-in SEM image shown in the inset indicates that the Ag nanocap is like an ellipsoidal semishell which is the thickest on the top. For comparison, the isolated Ag nanohole structure was fabricated by sonicating the evaporated sample in ethanol for about 30s to release the Ag nanocaps with the PS nanospheres and then rinsing with deionized water for several times. The isolated Ag nanocaps structure was fabricated by gently lifting them from their growth substrate with a double-sided tape.

For SERS spectra measurements, a 10 μL droplet of 1 μM R6G aqueous solution was dropped on the samples using an accurate pipette, and then dried in air at ambient temperature to obtain a uniform molecule deposition over an area of about 10 mm^2. The Raman scattering spectra were taken with a confocal microscopic Raman spectrometer (HORIBA Jobin Yvon LABRAM-HR). The samples were excited by a 785 nm semiconductor laser with about 0.45mW power through a 50× (N.A. 0.5) objective and the Raman signal was collected through the same objective in a backscattering geometry which is the same as that in ref. [16]. The integration time was 10s.

To investigate the electric field distribution and enhancement of the Ag nanocap-nanohole pairs, numerical simulations were performed using the three-dimensional finite-difference time-domain method (Lumerical FDTD Solutions). The boundary conditions of the simulation domain are perfectly matched layer absorbing boundaries. The calculation region is 2×2×1.5 μm^3, and the cell size is

UU IR Author Manuscript

$2\times2\times1$ nm^3. A linearly polarized plane wave with 785 nm wavelength illuminates the sample from the upper side. In order to closely match the experimental condition, the Ag nanocap was modeled as half of an ellipsoid shell with a concentric PS nanosphere core [15 17]. The radius of the core was set to 100nm, corresponding to that of the PS nanospheres used in the experiments. The thickest Ag layer on the top of the nanocap was set the same as that formed on the glass substrate; meanwhile the thinnest Ag layer on the edge of the nanocap was set to 15nm. The dielectric constants of the PS nanosphere was 1.6, while the dielectric constants of glass and Ag were based on the experimental data of ref. [18]. Since the Ag nanocap-nanohole pairs are many diameters apart on average, we ignored the interaction between each pair in the simulations.

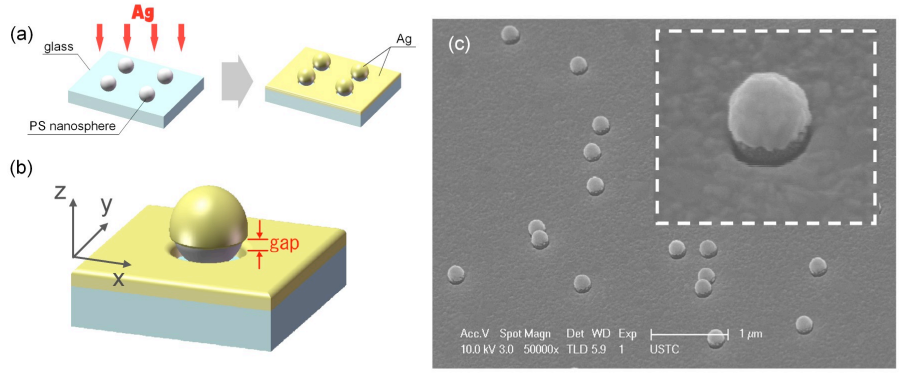

Figure 1. (a) Fabrication procedure for randomly spaced arrays of Ag nanocup-nanohole pairs. (b) Schematic illustration of a single Ag nanocup-nanohole pair. (c) 45° SEM images of the randomly spaced Ag nanocup-nanohole pairs. The inset is a zoomed-in 45° SEM image of a single Ag nanocup-nanohole pair.

Results and discussion

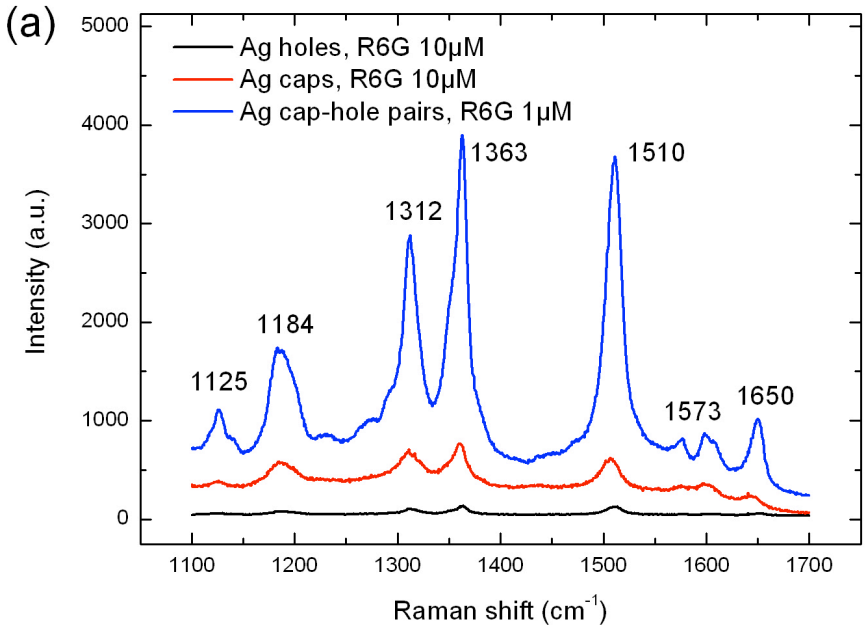

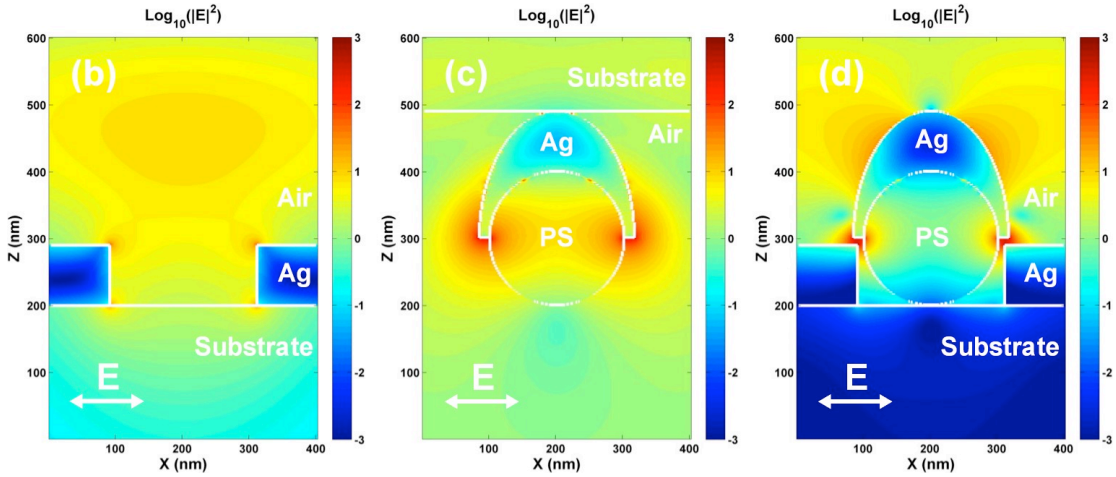

Figure 2. (a) Raman spectra of isolated Ag nanoholes (black), isolated Ag nanocaps (red) and the combined Ag nanocap-nanohole system (blue) with a Ag layer of 90 nm. (b)~(d) The corresponding simulated electric field distribution $Log_{10}|E|^2$ of the three structures. All structures were illuminated by normally incident light with 785 nm wavelength.

	Hole	Cap	Cap-hole
Maximum of $\|E\|^2$	183	2244	4756
Maximum of G_{SERS}	1.4×10^4	9.1×10^5	6.4×10^6
Hot spot number	0	84	172

Table 1. The maximum of electric field intensity and Raman gain G_{SERS} and the hot spot number calculated from the three structures (isolated Ag nanoholes, isolated Ag nanocaps and the combined Ag nanocap-nanohole system with a Ag layer of 90 nm), respectively.

The SERS performance of the combined Ag nanocap-nanohole system with an Ag layer of 90 nm (i.e. gap of 10 nm) is shown in Fig. 2 (a). For comparison, the Raman spectra from the isolated Ag nanocap and Ag nanohole structures were also performed (in order to achieve measurable Raman spectra we use 10 μM R6G aqueous solution in these two cases). From Fig. 2, obviously the combined system provides more than one order of magnitude greater SERS signal than from either of the isolated structures. The greater SERS signal of the combined system can be attributed to the enhanced electric field induced by the plasmonic coupling effect in the gap.

To further understand the electric mechanism of this coupling effect, the steady state field distributions of each structure were calculated by FDTD method, shown in Fig. 2(b)~(d). The maximum of electric field intensity and Raman gain (G_{SERS}) and the hot spot number derived from the simulation are performed in Tab. 1. As is generally agreed, the G_{SERS} can be expressed as [6 7 21,22]

$$G_{\mathrm{SERS}} \propto \left|\frac{E_{loc}(\lambda_{exc})}{E_{inc}(\lambda_{exc})}\right|^2 \left|\frac{E_{loc}(\lambda_{Raman})}{E_{inc}(\lambda_{Raman})}\right|^2$$

Where $E_{inc}(\lambda_{exc})$ and $E_{inc}(\lambda_{Raman})$ are the incident field and Raman emission field without enhancement, $E_{loc}(\lambda_{exc})$ and $E_{loc}(\lambda_{Raman})$ are the enhanced electric field at the incident and scattered wavelength. Ignoring the vectorial nature of the field and the tensorial properties of the Raman polarizability, G_{SERS} is roughly proportional to the fourth power of the electric field enhancement. A hot spot is defined as the point where the G_{SERS} is larger than a G_{SERS} threshold (10^5) [22]. The dimension of a single hot spot is the same with our simulation cell size. This enables the statistics of the hot spot number in the entire simulation region. It should be noted that the G_{SERS} and hot spot number are all collected from the structure surface to match the experimental situation that the analyte were adsorbed on the substrate surface for SERS detection.

From Fig. 2(b) and (c), both the isolated Ag nanocap and Ag nanohole support localized surface plasmons (LSPs) at their corners. When they are combined together, their LSPs interact, resulting in a plasmonic coupling effect which can greatly enhance the EM field and localize it into the small volume of the nano-scale gap. It provides much more hot spots and larger G_{SERS} maximum than the isolated structures, leading to the significant SERS effect.

UU IR Author Manuscript

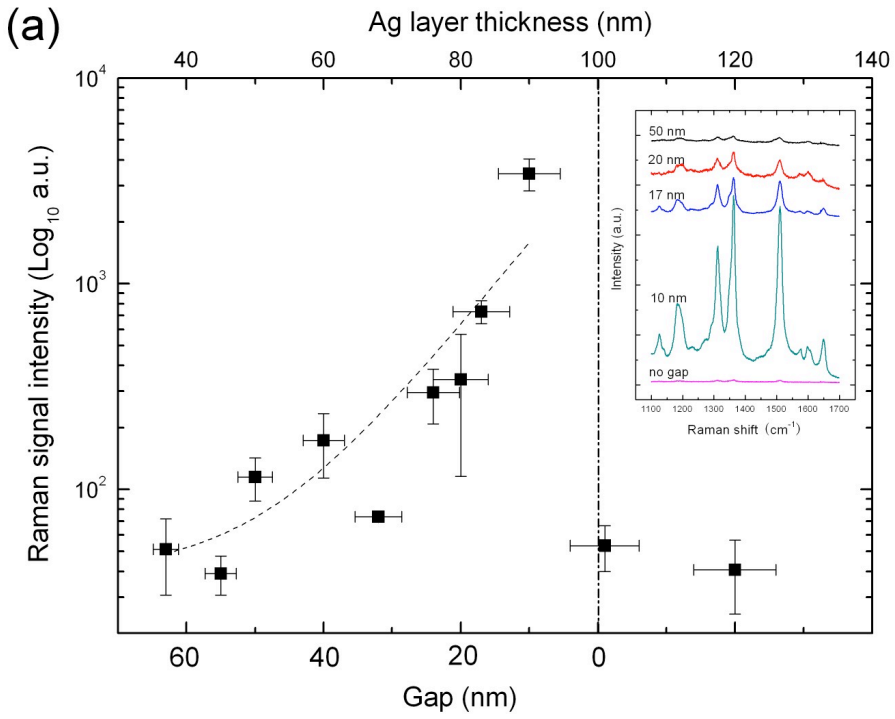

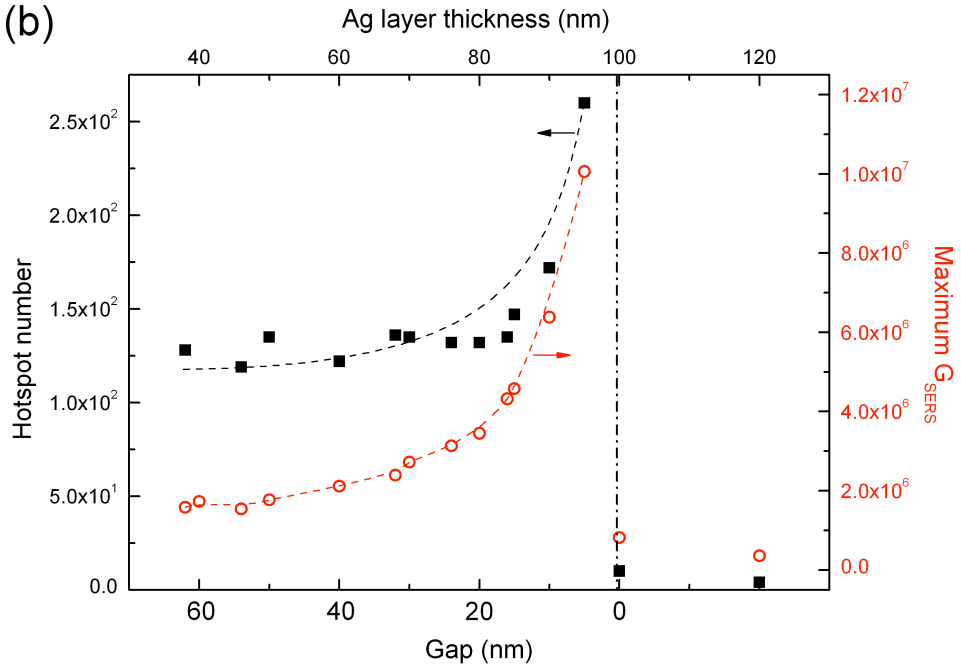

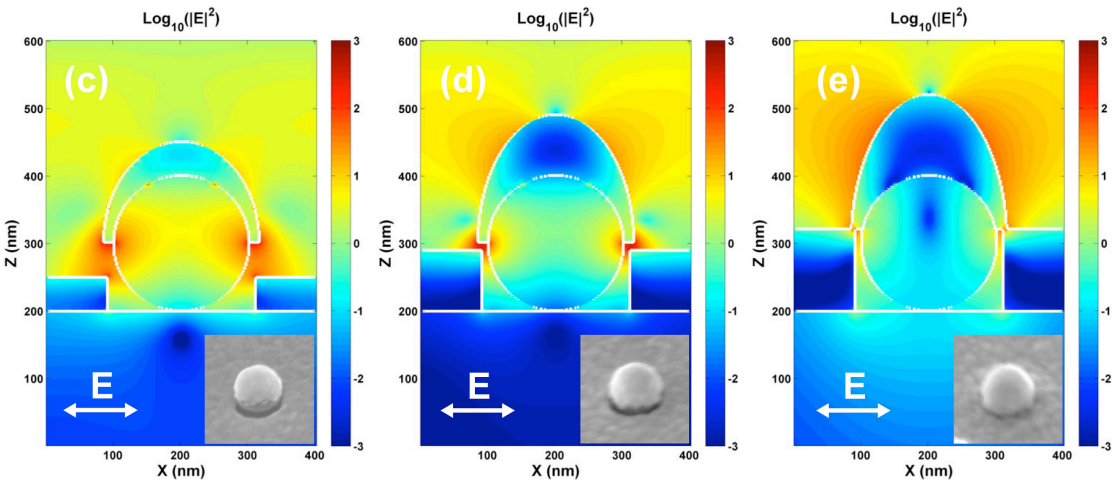

Figure 3. (a) Plot of the Raman signal intensity derived from the 1363 cm^{-1} peak as a function of the gap and corresponding Ag layer thickness. The inset shows the Raman spectra for a series of gaps: 50 nm-gap (black), 20 nm-gap (red), 17 nm-gap (blue), 10 nm-gap (green), no gap (pink). (b) Simulated hot spot number and maximum G_{SERS} as a function of the gap and corresponding Ag layer thickness. (c)~(e) Simulated electric field distribution $Log_{10}|E|^2$ and corresponding 45° SEM images of the Ag nanocap-nanohole pairs with three typical gaps: (c) 50 nm-gap, (d) 10 nm-gap and (e) no gap. All of them were illuminated by normally incident light with 785 nm wavelength.

Furthermore, our fabrication method facilitates control over the gap size, which has strong influence on SERS enhancement. The separation between the nanohole and the nanocap is determined by the thickness of the evaporated Ag layer. The thicker the Ag layer, the smaller the gap. When the thickness exceeds the radius of the PS nanosphere, the nanocap is joined with the nanohole and the gap vanishes. Fig. 3 (a) shows the Raman signal intensity as a function of the gap size and corresponding Ag layer thickness. These measurements were performed under the same conditions and derived from the 1363cm^{-1} peak of the Raman spectra. We also plot the maximum of G_{SERS} and the hot spot number as a function of the gap size in Fig. 3(b).

From Fig. 3, for the gap larger than 50nm (i.e. Ag layer thickness less than 50nm), the Raman signal is not significantly improved over that obtained from isolated structures, representing weak field enhancement within the gap. It means that the plasmon interaction is quite weak in such case, due to the field attenuation deviating from either side of the gap. The calculated field distribution also confirms this point (seen as Fig. 3(c)). When the gap size is decreased to ~50nm or less, the plasmon interaction effect appears. The hot spot number and the maximum of G_{SERS} start to increase drastically. As a result the Raman signal intensity starts to increase. It is similar to that in the nano-antenna gap [23] or particle-film coupled system [24]. In our experiments, the Raman signals of the 10 nm-gap (i.e. 90 nm-thick Ag layer) system reaches about thirty-fold greater than that of the 50 nm-gap case. This is the strong interaction case: due to the small distance between the nanocap and nanohole, LSPs from each structure are strongly coupled and thereby significantly enhance the field in the gap[25], providing a great number of hot spots to active the Raman molecule (seen

UU IR Author Manuscript

as Fig. 3(d)). When the Ag layer thickness is further increased to over 100 nm, the edges of the Ag nanocap and the Ag nanohole are connected together. So the structure can be analogized to a roughness on a continuous Ag layer with no LSP coupling effect (seen as Fig. 3(e)). Therefore the hot spot number and the maximum of G_{SERS} decline dramatically. As a result, the Raman signal falls nearly two orders of magnitude lower than that of the optimal case.

The SERS enhancement factor (EF) value can be calculated from the experiment measurements using the methods put forth by Van Duyune[19 20]. We chose the Raman band at 1363 cm^{-1} to measure the signal intensity and used the hot spot number discussed above to derive the number of excited Raman molecules in SERS process. The result shows the Ag nanocap-nanohole coupling structure can provide a peak EF of 1.1×10^{8} with the optimal gap size.

Conclusion

In conclusion, we have proposed a composite plasmonic structure consisting of coupled Ag nanocap-nanohole pairs. This structure can be fabricated through a simple physical method. Because of the plasmonic coupling effect, localized electric fields can be significantly enhanced within the nano-scale gaps in the combined systems, as indicated by the SERS measurements and numerical simulations. We demonstrated that the intensity of SERS signals can be effectively controlled by the gap. When the gap size is 10 nm, its SERS EF under 785 nm excitation can reach 1.1×10^{8}, which is much higher than that of the isolated structures.

This work provides a facile top-down fabrication method for SERS substrate with high EF in NIR wavelength. It also enables a more compact distribution of the coupled units, even periodical arrangement, which is expect to provide greater Raman signals towards the goal of reproducible single-molecule SERS detection. Moreover, by offering an accessible means to produce high electric field enhancement with nano-scale gaps, we anticipate that this approach will enable novel plasmonic applications in many other areas, such as fluorescence enhancement and nano-antennas.

Acknowledgments

This work is supported by National Basic Research Program (973 Program) of China under Grant No. 2012CB921900, the Key Program of National Natural Science Foundation of China No. 61036005 and National Natural Science Foundation of China No. 11074241, 11004182

Reference

1 Nie, S. & Emory, S. R. Probing Single Molecules and Single Nanoparticles by Surface-Enhanced Raman Scattering. *Science* **275**, 1102-1106, doi:10.1126/science.275.5303.1102 (1997).

2 Winkler, K., Kaminska, A., Wojciechowski, T., Holyst, R. & Fialkowski, M. Gold

UU IR Author Manuscript

Micro-Flowers: One-Step Fabrication of Efficient, Highly Reproducible Surface-Enhanced Raman Spectroscopy Platform. *Plasmonics*, 1-8, doi:10.1007/s11468-011-9253-0 (2011).

3 Yi, M. *et al.* Plasmonic Interaction Between Silver Nano-Cubes and a Silver Ground Plane Studied by Surface-Enhanced Raman Scattering. *Plasmonics*, 1-5, doi:10.1007/s11468-011-9230-7 (2011).

4 Michaels, A. M., Nirmal, M. & Brus, L. E. Surface Enhanced Raman Spectroscopy of Individual Rhodamine 6G Molecules on Large Ag Nanocrystals. *Journal of the American Chemical Society* **121**, 9932-9939, doi:10.1021/ja992128q (1999).

5 Otto, A. & et al. Surface-enhanced Raman scattering. *Journal of Physics: Condensed Matter* **4**, 1143 (1992).

6 Moskovits, M. Surface-enhanced spectroscopy. *Rev Mod Phys* **57**, 783 (1985).

7 Metiu, H. & Das, P. The Electromagnetic Theory of Surface Enhanced Spectroscopy. *Annual Review of Physical Chemistry* **35**, 507-536, doi:10.1146/annurev.pc.35.100184.002451 (1984).

8 Ye, J. *et al.* Tuning plasmonic interaction between gold nanorings and a gold film for surface enhanced Raman scattering. *Appl. Phys. Lett.* **97**, 163106-163103, doi:10.1063/1.3504187 (2010).

9 Im, H., Bantz, K. C., Lindquist, N. C., Haynes, C. L. & Oh, S.-H. Vertically Oriented Sub-10-nm Plasmonic Nanogap Arrays. *Nano Letters* **10**, 2231-2236, doi:10.1021/nl1012085 (2010).

10 Wei, H., Håkanson, U., Yang, Z., Höök, F. & Xu, H. Individual Nanometer Hole-Particle Pairs for Surface-Enhanced Raman Scattering. *Small* **4**, 1296-1300 (2008).

11 Xiaolei, W. & et al. Tunable plasmonic coupling between silver nano-cubes and silver nano-hole arrays. *Nanotechnology* **22**, 085203 (2011).

12 Lu, Y., Liu, G. L., Kim, J., Mejia, Y. X. & Lee, L. P. Nanophotonic Crescent Moon Structures with Sharp Edge for Ultrasensitive Biomolecular Detection by Local Electromagnetic Field Enhancement Effect. *Nano Letters* **5**, 119-124, doi:10.1021/nl048232+ (2004).

13 Kneipp, K. *et al.* Detection and identification of a single DNA base molecule using surface-enhanced Raman scattering (SERS). *Physical Review E* **57**, R6281 (1998).

14 Love, J. C., Gates, B. D., Wolfe, D. B., Paul, K. E. & Whitesides, G. M. Fabrication and Wetting Properties of Metallic Half-Shells with Submicron Diameters. *Nano Letters* **2**, 891-894, doi:10.1021/nl025633l (2002).

15 Zhang, Y., Barhoumi, A., Lassiter, J. B. & Halas, N. J. Orientation-Preserving Transfer and Directional Light Scattering from Individual Light-Bending Nanoparticles. *Nano Letters*, null-null, doi:10.1021/nl2008357 (2011).

16 Wei, H. *et al.* Polarization Dependence of Surface-Enhanced Raman Scattering in Gold Nanoparticle−Nanowire Systems. *Nano Letters* **8**, 2497-2502, doi:10.1021/nl8015297 (2008).

17 Mirin, N. A. & Halas, N. J. Light-Bending Nanoparticles. *Nano Letters* **9**, 1255-1259, doi:10.1021/nl900208z (2009).

18 Palik, E. D. Handbook of Optical Constants of Solids. *Elsevier* (1998).

19 Van Duyne, R. P., Hulteen, J. C. & Treichel, D. A. Atomic force microscopy and surface-enhanced Raman spectroscopy. I. Ag island films and Ag film over polymer nanosphere surfaces supported on glass. *The Journal of Chemical Physics* **99**, 2101-2115, doi:10.1063/1.465276 (1993).

20 Lin, W.-C. *et al.* Controlling SERS intensity by tuning the size and height of a silver nanoparticle array. *Applied Physics A: Materials Science & Processing* **101**, 185-189, doi:10.1007/s00339-010-5777-y (2010).

21 Moskovits, M. in *Surface-Enhanced Raman Scattering* Vol. 103 *Topics in Applied Physics* (eds Katrin Kneipp, Martin Moskovits, & Harald Kneipp) 1-17 (Springer Berlin / Heidelberg, 2006).

22 Wu, H.-Y. & Cunningham, B. T. Plasmonic coupling of SiO[sub 2]--Ag ``post-cap'' nanostructures and silver film for surface enhanced Raman scattering. *Appl. Phys. Lett.* **98**, 153103-153103, doi:10.1063/1.3555342 (2011).

23 Yamaguchi, K. & et al. Electric Field Enhancement of Nano Gap of Silver Prisms. *Chinese Physics Letters* **24**, 2934 (2007).

24 Lévêque, G. & Martin, O. J. F. Optical interactions in a plasmonic particle coupled to a metallic film. *Opt. Express* **14**, 9971-9981 (2006).

25 Zhu, W., Banaee, M. G., Wang, D., Chu, Y. & Crozier, K. B. Lithographically Fabricated Optical Antennas with Gaps Well Below 10 nm. *Small* **7**, 1761-1766, doi:10.1002/smll.201100371 (2011).

UU IR Author Manuscript